A Simple All-Fiber Solc Filter Based on 45°-Tilted Fiber Gratings

Zhikun Xing, Xi Guo, Huabao Qin, Wei Zhang, Qizhen Sun, Kaiming Zhou, Zhijun Yan, Deming Liu, and Lin Zhang

Abstract—**A simple all-fiber Solc filter (AFSF), which consists of two 45°-tilted fiber gratings (45°-TFGs) UV-inscribed in the polarization-maintaining fiber (PMF) and a series of PMF cavities, is proposed and demonstrated. The performance of the proposed filter has been theoretically simulated and experimentally verified. Both the simulated and experimental results show that the bandwidth of the filter could be tuned by the PMF sub-cavity length and the number of PMF cavities. And the free spectral range (FSR) only depends on the sub-cavity length. As a proof of that, the bandwidths of AFSF with different number of PMF sub-cavity (N=2, N=3, N=4) and the same PMF sub-cavity length of 30cm are 4 nm, 2.6nm, and 2nm, respectively. The FSRs of 3-stage AFSF with different PMF sub-cavity length (L=20 cm and L=40 cm) are 15.3 nm and 7.97 nm, respectively. Furthermore, we have also investigated the tunability of the AFSF by controlling the temperature of PMF cavity with a tuning sensitivity around 1.205 nm/℃. Compared with existing fiber-optic Solc filters, the AFSF with prominent advantages such as extremely simple and robust structure, thermal tunability in wavelength, and low cost will bring a bright future for applications in optical communication and sensing systems.**

Index Terms—**Solc filter, 45°-tilted fiber gratings, all-fiber device, birefringence.**

I. INTRODUCTION

WITH the rapidly increased demand for optical signal processing and optical communication systems, the development of birefringent filter, as a key component with the well-known characteristics of spectral flexibility and narrow bandwidth, has attracted growing research interest. The birefringent filters include two classical types: Lyot filter [1] and Solc filter [2]. Compared with the Lyot filter, the Solc filter has attracted more attention and widespread applications by virtue of its simple configuration and low loss. A variety of techniques have been proposed to realize Solc filter function such as the use of periodically poled lithium niobate (PPLN) based on the electro-optic effect [3-5], photovoltaic effect [6], UV-light illumination [7,8], and optical waveguide [9-11]. However, all these reported Solc filters are built only in the bulk form, resulting in the chunky structure and low integration. In addition, these filters need external electric field or UV light to assist with work, which adds the operative difficulties in practical use. With an aim to build in-fiber filters better applied into all-fiber system, several optical birefringent filters based on single-mode fibers (SMFs) [12-14], high-birefringence fibers (HBFs) [15-18], and elliptical-core spun fiber (ECSF) [19,20] have been widely investigated to replace the chunky structure. Nevertheless, these fiber-optic Solc and Solc-sagnac filters are still constructed using bulk components, which will induce high insertion loss and coupling problems.

Tilted fiber gratings (TFGs) were found good polarization properties when the tilted angle is exactly 45° with respect to the normal of fiber axis, which could function as ideal in-fiber polarizers. In our previous work, the 45°-tilted fiber grating (45°-TFG) was achieved to be inscribed into the polarization-maintaining fibers (PMFs) along the fast or slow axis [21], which may have promising applications as a linear polarized light output with prominent merits, including high polarization-extinction-ratio (PER), low insertion loss, and nice compatibility with other fiber devices. In this paper, we propose and experimentally demonstrate a simple all-fiber Solc filter (AFSF) based on concatenated 45°-TFGs UV-inscribed in PMF and a series of PMF cavities. The numerical simulations show that the bandwidth of the proposed filter could be easily controlled by utilizing appropriate sections of PMF cavities, and the free spectral range (FSR) is PMF cavity length dependent. In the experiment, we have investigated the filter characteristics with different PMF sub-cavity lengths and number of PMF sub-cavities. Additionally, the thermal tunability of AFSF has been also presented with a tuning
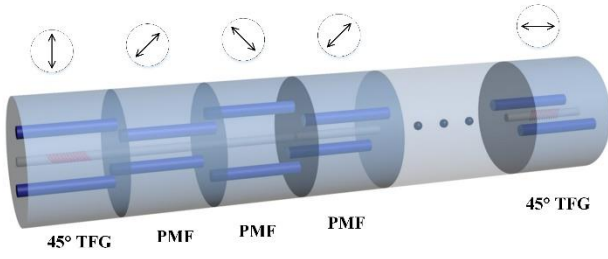
Fig. 1. Schematic configuration of a multistage AFSF.

sensitivity up to 1.205 nm/℃. Compared with the other reported fiber-optic Solc filters [17-20], the proposed filter can achieve desirable bandwidth and FSR respectively, giving more freedom in tailoring the transmission characteristics, and also presents relatively low insertion loss, more desirable bandwidth with shorter PMF length, nice compatibility with other fiber devices, which has great potential for applications in optical communication, sensing and laser systems.

II. THEORY AND PRINCIPLE

The classical Solc filter is composed of a pile of identical retardation plates placed between two orthogonal polarizers, where the set of retarders have the same, but alternating orientation. In our proposed AFSF, several sections of PMFs (PM1550 fiber, YOFC) are employed as retarders, of which the beat length is 2 mm at 1550 nm, corresponding to $\Delta n = 7.75 \times 10^{-4}$, and two 45°-TFGs inscribed into the PMFs along slow axis are used as the linear polarizers. The schematic configuration of a multistage AFSF is illustrated in Fig. 1, where all the components are fusion spliced to each other. The working principle of the AFSF is described as follows: the input light passing the first 45°-TFG becomes linearly polarized and then enters the PMF cavities, which will be subsequently resolved into two beams propagating along the fast- and slow-axis of the PMF, respectively. The birefringence of the PMF will induce a phase difference between these two beams; thus when they finally arrive at the second 45°-TFG, the combined beam will generate interference and only in-phase light can pass through the second 45°-TFG. To simplify the calculation, the slow axis of the PMF that is hosting the first 45°-TFG is defined as x-axis, and thus the second is perpendicular to x-axis. By applying the transfer matrix method, the N-stage Solc filter can be described as:

$$G = \begin{bmatrix} 0 & 0 \\ 0 & 1 \end{bmatrix} R(-\theta) W(\delta)^{j} \left(R(2\theta) W(\delta) R(-2\theta) W(\delta) \right)^{K} R(\theta) \begin{bmatrix} 1 & 0 \\ 0 & 0 \end{bmatrix}$$

(1)

where K=(N-1)/2, j=1 when the AFSF is constructed with odd sections of PMF cavities, or K=N/2, j=0 with even sections of PMF cavities. Besides, $R(\theta)$ is the rotation matrix, and $W(\delta)$ represents the Jones matrix of a retarder with its fast axis in x-axis direction, which are given respectively as follows:

$$R(\theta) = \begin{bmatrix} \cos\theta & \sin\theta \\ -\sin\theta & \cos\theta \end{bmatrix}$$

(2)

$$W(\delta) = \begin{bmatrix} 1 & 0 \\ 0 & e^{i\frac{2\pi}{\lambda}\Delta nL} \end{bmatrix}$$

(3)

here θ is the azimuth angle, which depends on the number N of PMF sections, λ is the working wavelength, Δn is the birefringence of PMF, and L is the length of PMF.

Due to the thermal effect on birefringence of PMF, the AFSF can achieve thermal tunability over a broad wavelength range by adjusting the temperature. Specifically, when the PMF cavity is under heating, the thermal expansion coefficient and thermal optical coefficient of PMF will be altered, and the total phase shift will change accordingly, resulting in the wavelength shifting. The thermal tunability of the AFSF can be expressed as [22]

$$\Delta\lambda = \lambda \left(\frac{dL}{LdT} + \frac{d\Delta n}{\Delta ndT} \right) \cdot \Delta T$$

(4)

where dL/(LdT) is the thermal expansion coefficient, and $d\Delta n/(\Delta ndT)$ is the thermal optical coefficient, which are both constants. From Eq. (4), the wavelength shift $\Delta\lambda$ is linearly proportional to the temperature variation ΔT.

III. SIMULATION AND DISCUSSION

The performance of the AFSF could be altered by changing the parameters of PMF cavities. Hence, theoretical transmission spectrum and its influencing factors in terms of section N, birefringence Δn, and sub-cavity length L have been explored as follows.

A. Filter Characteristics with the Section N

In the simulation, the initial parameters are chosen as follows: L = 30 cm, Δn = 7.75×10^{-4}. The simulated transmission spectrum with different value of N is shown in Fig. 2(a), from which we can see that the bandwidth of the simulated transmission spectrum is inversely proportional to the value of N, since the 3 dB linewidth decreases with the increase of PMF sections. It can be also concluded from Fig. 2(b) that the FSR of the AFSF is independent of the value of N, given that the FSR remains unchanged while N is enhancing.
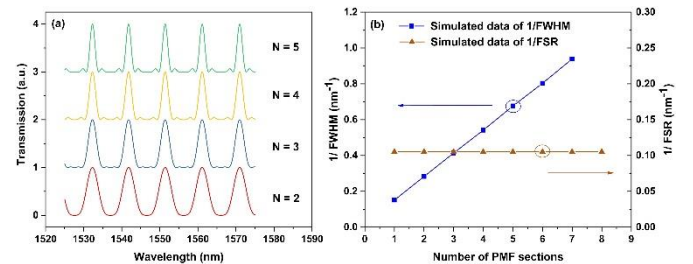

Fig. 2. Filter characteristics with the section N.

B. Filter Characteristics with the Birefringence Δn

The simulated transmission spectrum with different birefringence Δn is depicted in Fig. 3(a). The initial parameters in the simulation are set as follows: $N = 3$, $L = 30$ cm. As shown in Fig. 3(a), when Δn increases, the FSR and 3 dB linewidth reduce. Furthermore, it can be seen in Fig. 3(b) that the FSR and bandwidth of the AFSF are both inversely proportional to the birefringence Δn.
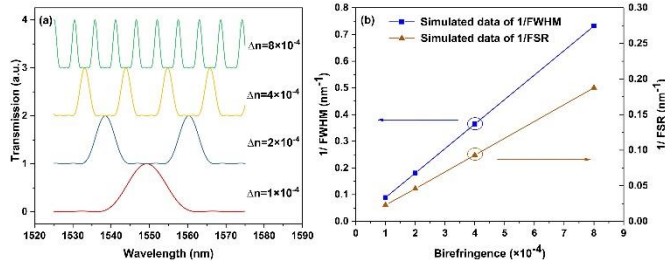

Fig. 3. Filter characteristics with the birefringence Δn.

C. Filter Characteristics with the Sub-cavity Length L

The transmission spectrum of the AFSF with four different PMF sub-cavity lengths is plotted in Fig. 4(a). It can be seen that the FSR and 3 dB linewidth enhance with the decreasing PMF length, while the section N and birefringence Δn remain constant. Fig. 4(b) illustrates the filter characteristics with PMF sub-cavity length L, which indicates that the FSR and bandwidth of the AFSF are both in inverse ratio to the PMF sub-cavity length.
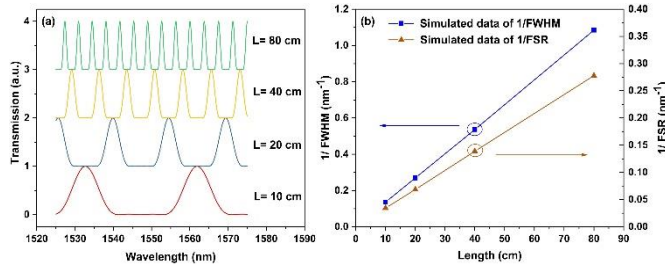

Fig. 4. Filter characteristics with the sub-cavity length L.

According to all aforementioned simulation results, we could conclude that the FSR and bandwidth of the AFSF will decrease simultaneously when the birefringence Δn and PMF sub-cavity length L enhance. In addition, the bandwidth can be controlled independently by selecting appropriate sections of PMF. So, we could design the FSR and bandwidth of the AFSF for requirement of various applications by choosing desired PMF sub-cavity length and number of PMF sub-cavity.

IV. EXPERIMENTAL VALIDATION

To verify the theoretical analysis and simulation results, we have demonstrated the AFSF and measured the transmission spectra with different PMF sub-cavity lengths and number of PMF sub-cavity. The experimental setup is illustrated in Fig. 5, in which an amplified spontaneous emission (ASE) is employed as a broadband light source (wavelength ranging from 1525 nm to 1575 nm) and an optical spectrum analyzer (OSA, AQ6375B)
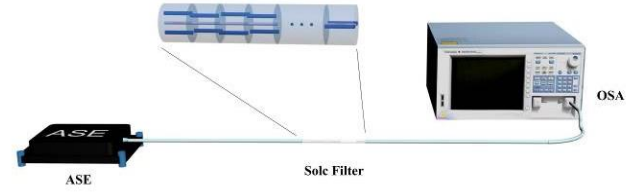

Fig. 5. Experimental setup for measuring the transmission spectrum of AFSF.

with a resolution of 0.05 nm is used to monitor the real-time transmission spectrum.

In the experiment, we have fabricated three AFSFs with different number of PMF sub-cavity (N=2, N=3, N=4) and the same PMF sub-cavity length of 30cm. The measured and simulated transmission spectra of three AFSFs are shown in Fig. 6(a)-(c). It can be seen that the experimental results are in good agreement with the simulated ones. And the bandwidth of filter decreases with the increasing number of PMF sub-cavity. The 3 dB linewidth in Fig. 6(a) is about 4 nm, while the one in Fig. 6(b) is about 2.6 nm and Fig. 6(c) about 2 nm. In addition, the FSR and extinction ratio (ER) of all the transmission spectrum are approximately 10 nm and 20 dB, respectively. Taking the fiber splices into account, the intrinsic insertion loss is about 3.5 dB. Fig. 6(d) presents the filter characteristics with different parameter N, which indicates that the bandwidth is inversely proportional to the section N, while the FSR is independent of N, showing good consistency with the simulation results.
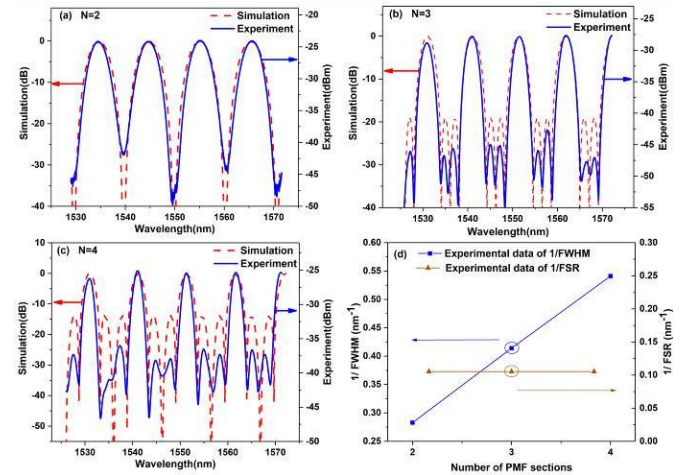

Fig. 6. Comparison between theoretical calculation and experimental results of the AFSF with (a) N = 2, (b) N = 3, (c) N = 4, and (d) filter characteristics with the section N.

Furthermore, we have also investigated experimentally the filter characteristics with different PMF sub-cavity cavity lengths (20 cm, 30 cm and 40 cm) and the same number of PMF sub-cavity (N=3). As revealed in Fig. 7(a)-(c), the 15.3 nm FSR with 20cm long PMF sub-cavity is twice as much as the 7.97 nm FSR with 40cm long PMF cavity. Fig. 7(d) plots the relationship between FSR, bandwidth, and PMF sub-cavity length, which could vividly lead us to conclude that the FSR and bandwidth of the AFSF are both in inverse ratio to the PMF length.
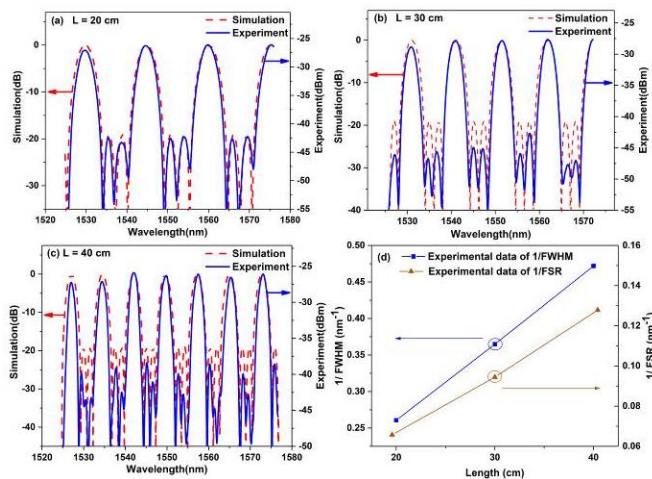
Fig. 7. Comparison between theoretical calculation and experimental results of the AFSF with (a) L = 20 cm, (b) L = 30 cm, (c) L = 40 cm, and (d) filter characteristics with the sub-cavity length L.

Moreover, the wavelength tunability of AFSF (N=2 and L=30 cm) has been tested by adjusting the temperature. The whole length of the PMF cavity was heated from 30℃ to 36℃ with an increment of 1℃ using a temperature controllable peltier, in which the wavelength of the filter could be tuned to cover the entire FSR, as shown in Fig.8(a). The wavelength shift is linearly proportion to the temperature with the tuning sensitivity of 1.205 nm/℃ (see in Fig.8(b)), which is in very good agreement with the theoretical result.
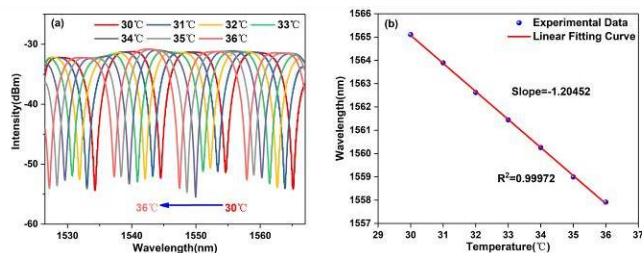

Fig. 8. Transmission spectrum and wavelength variation under thermal tuning.

V. CONCLUSION

In summary, we proposed and experimentally demonstrated an AFSF with a simple configuration utilizing several sections of PMF and two 45°-TFGs UV-inscribed in the PMF. The experimental results are in good accordance with the simulation results, which illustrate that the FSR and bandwidth of the proposed filter will decrease simultaneously when the birefringence Δn and PMF sub-cavity length L enhance. Furthermore, the bandwidth can be controlled independently by selecting appropriate sections of PMFs, giving more freedom in tailoring the transmission characteristics. In addition, the AFSF can achieve wavelength tunability based on the thermal effect with a tuning sensitivity up to 1.205 nm/℃. The proposed filter with prominent merits such as extremely simple and robust structure, narrow bandwidth, spectral flexibility, and low cost is highly desirable for in-fiber laser, spectral imaging, optical communication and sensing systems.

REFERENCES

[1] J. W. Evans, "The birefringent filter," *J. Opt. Soc. Amer.,* vol. 39, no. 3, pp. 229–242, Mar. 1949.

[2] I. Šolc, "Birefringent chain filters," *J. Opt. Soc. Amer.,* vol. 55, no. 6, pp. 621–625, Jun. 1965.

[3] X. F. Chen, J. H. Shi, Y. P. Chen, Y. M. Zhu, Y. X. Xia, and Y. L. Chen, "Electro-optic Solc-type periodically poled wavelength filter in lithium niobate," *Opt. Lett.,* vol. 28, no. 21, pp. 2115-2117, 2003.

[4] Rabia. Eyal, and A. Arie, "Duty cycle dependence of a periodically poled LiNbO3-based electro-optic Solc filter," *Appl. Opt.,* vol. 45, no. 3, pp. 540–545, 2006.

[5] K. Liu, J. Shi, and X. Chen, "Electro-optical flat-top bandpass Solc-type filter in periodically poled lithium niobate," *Opt. Lett.,* vol. 34, no. 7, pp. 1051–1053, 2009.

[6] Chen L, Shi J, Chen X, and Xia. Y, "Photovoltaic effect in a periodically poled lithium niobate Solc-type wavelength filter," *Appl. Phys. Lett.,* vol. 88, no. 12, pp. 121118–121120, 2006.

[7] Shi J, Wang J, Chen L, Chen X, and Xia. Y, "Tunable Solc-type filter in periodically poled LiNbO3 by UV-light illumination," *Opt. Express,* vol. 14, no. 13, pp. 6279–6284, 2006.

[8] Y.L. Lee, N.E. Yu, C.-S. Kee, D.-K. Ko, Y.-C. Noh, B.-A. Yu, W. Shin, T.-J. Eom, K. Oh, and J. Lee, "All-optical wavelength tuning in Solc filter based on Ti: PPLN waveguide," *Electron. Lett.*, vol. 44, no. 1, pp. 30–31, 2008.

[9] Y. L. Lee, N. E. Yu, C.-S. Kee, D.-K. Ko, J. Lee, B.-A. Yu, W. Shin, T. J. Eom, and Y.-C. Noh, "Wavelength filtering characteristics of Šolc filter based on Ti: PPLN channel waveguide," *Opt. Lett.,* vol. 32, no. 19, pp. 2813–2815, 2007.

[10] C. Y. Huang, C. H. Lin, Y. H. Chen, and Y. C. Huang, "Electro-optic Ti: PPLN waveguide as efficient optical wavelength filter and polarization mode converter," *Opt. Express,* vol. 15, no. 5, pp. 2548–2554, 2007.

[11] Y. L. Lee, N. E. Yu, C.-S. Kee, D.-K. Ko, Y.-C. Noh, B.-A. Yu, W. Shin, T. J. Eom, J. Lee, "Waveguide-Type Wavelength-Tunable Solc Filter in a Periodically Poled Ti: LiNbO3 Waveguide," *IEEE Photon. Technol. Lett.*, vol. 19, no. 17, pp. 1505–1507, 2007.

[12] J. H. Osório and C. M. B. Cordeiro, "Optical sensor based on two in-series birefringent optical fibers," *Appl. Opt.,* vol. 52, no. 20, pp. 4915–4921, 2013.

[13] M. Johnson, "Single-mode-fiber birefringent filters," *Opt. Lett.,* vol. 5, no. 4, pp. 142–144, 1980.

[14] K. Okamoto, J. Noda, and H. Miyazawa, "Fibre-optic Solc filter for use in Raman amplification of light," *Electron. Lett.*, vol. 21, no. 3, pp. 90–91, 1985.

[15] S. Li, K. Chiang, and W. Gambling, "Gain flattening of an erbium-doped fiber amplifier using a high-birefringence fiber loop mirror," *IEEE Photon. Technol. Lett.*, vol. 13, no. 9, pp. 942–944, 2001.

[16] Y. Liu, B. Liu, X. Feng, W. Zhang, G. Zhou, S. Yuan, G. Kai, and X. Dong, "High-birefringence fiber loop mirrors and their applications as sensors," *Appl. Opt.,* vol. 44, no. 12, pp. 2382–2390, 2005.

[17] D. Feng and J. Sun, "Optical single sideband modulation based on a high-order birefringent filter using cascaded Solc-Sagnac and Lyot-Sagnac loops," *Opt. Lett.,* vol. 41, no. 15, pp. 3659–3662, 2016.

[18] Bo Huang, and Xuewen Shu, "Highly Sensitive Twist Sensor Based on Temperature and Strain-Independent Fiber Lyot Filter," *J. Lightw. Technol.,* vol. 35, no. 10, pp. 2026–2031, 2017.

[19] C. Sun, S. Ye, and S. Jian, "Solc-Like Tunable Birefringent Fiber Filter Based on Elliptical-Core Spun Fiber," *IEEE Photon. Technol. Lett.*, vol. 29, no. 12, pp. 1031–1034, 2017.

[20] Chunran, Sun, W. Muguang, and J. Shuisheng, "Experimental and theoretical study of the in- fiber twist sensor based on quasi-fan Solc structure filter," *Opt. Express,* vol. 25, no. 17, pp. 19955-19965, 2017.

[21] Z. Yan, K. Zhou, and L. Zhang, "In-fiber linear polarizer based on UV-inscribed 45 tilted grating in polarization maintaining fiber," *Opt. Lett.,* vol. 37, pp. 3819–3821, no. 18, 2012.

[22] Z. Yan, H. Wang, K. Zhou, Y. Wang, W. Zhao, and L. Zhang, "Broadband Tunable All-Fiber Polarization Interference Filter Based on 45° Tilted Fiber Gratings" *J. Lightw. Technol.,* vol. 31, no. 1, pp. 94-98, 2013.